

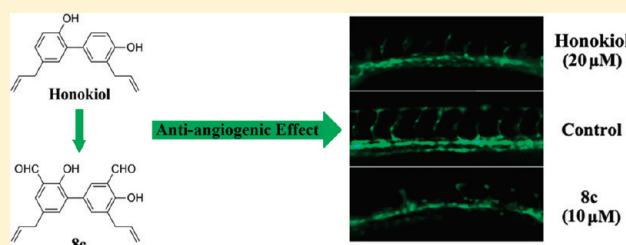
Structural Modification of Honokiol, a Biphenyl Occurring in *Magnolia officinalis*: the Evaluation of Honokiol Analogues as Inhibitors of Angiogenesis and for Their Cytotoxicity and Structure–Activity Relationship

Liang Ma,[†] Jinying Chen,[†] Xuwei Wang,[†] Xiaolin Liang, Youfu Luo, Wei Zhu, Tianen Wang, Ming Peng, Shucui Li, Shi Jie, Aihua Peng, Yuquan Wei, and Lijuan Chen*

State Key Laboratory of Biotherapy, West China Hospital, West China Medical School, Sichuan University, Keyuan Road 4, Gaopeng Street, Chengdu 610041, China

S Supporting Information

ABSTRACT: Honokiol, widely known as an antitumor agent, has been used as an antiangiogenesis drug lead. In this paper, 47 honokiol analogues and derivatives were investigated for their antiangiogenic activity by application of the transgenic zebrafish screening model, antiproliferative and cytotoxic activity against HUVECs, and three tumor cell lines by MTT assay. 3',5-Diallyl-2,4'-dihydroxy-[1,1'-biphenyl]-3,5'-dicarbaldehyde (**8c**) was found to suppress the newly grown segmental vessels from the dorsal aorta of zebrafish and prevent inappropriate vascularization as well as exhibit more potent inhibitory effects on the proliferation of HUVECs, A549, HepG2, and LL/2 cells (IC_{50} = 15.1, 30.2, 10.7, and 21.7 μ M, respectively) than honokiol (IC_{50} = 52.6, 35.0, 16.5, and 65.4 μ M, respectively). Analogue **8c** also effectively inhibited the migration and capillary-like tube formation of HUVECs in vitro. The antiangiogenic effect and antiproliferative activity of these structurally modified honokiol analogues and derivatives have led to the establishment of a structure–activity relationship.



INTRODUCTION

Angiogenesis is a critical step for tumor cell proliferation, invasion, and metastasis in several solid tumors and hematological malignancies.¹ Tumor growth depends on angiogenesis, i.e., the recruitment of new blood vessels from pre-existing vasculature.² Without the development and progression of new blood vessels, tumors cannot deteriorate beyond a critical size or metastasize to other organs.³ Angiogenesis also is a complicated multistep process involving endothelial cell (EC) activation, invasion, migration, proliferation, tube formation, and finally capillary network formation.⁴

The zebrafish (*Danio rerio*) screening model for antiangiogenesis has first emerged as an important vertebrate model organism in the 1970s and has since been increasingly applied to the study of human diseases.⁵ The advantages of zebrafish as a valid tumor model system for antiangiogenesis screening are well documented, including its low cost, easy maintenance, rapid generation time (about three months), large clutch size (number of offspring), the presence of transparent embryos, and ex utero embryonic development.⁶ By the application of transgenesis, particular ECs of zebrafish could be easily observed for gene expression or cellular morphology before and after drug exposure. In the transgenic zebrafish model, fetal liver kinase-1 (*flk-1*) enhanced green fluorescent proteins (GFP)-nuclear localization signal (NLS) transgenics express GFP in the nucleus of ECs and friend

leukemia integration-1 (*fli-1*) enhanced GFP transgenics express GFP in the entire ECs, facilitating imaging of the vascular anatomy.⁷

ECs play pivotal roles in a range of physiological processes such as angiogenesis and as the selective blood barrier. They are also involved in many pathophysiological events including arterial disease and cancer development. One of the principal targets of antiangiogenic therapy is genetically stable, nontransformed ECs which are less prone to acquire drug resistance.⁸ When tumor cells secrete pro-angiogenic growth factors that bind to receptors on dormant ECs, leading to ECs activation, stimulation, vasodilatation, and an up-regulation of vessel permeability, these activated ECs could rapidly detach from the extracellular matrix and basement membrane. They further migrate, proliferate to sprout and self-assemble into new branches, followed by the formation of a new basement membrane.^{9,10} Therefore, inhibition of the proliferation, migration, and tube formation of ECs might be an effective therapy for suppressing tumor progression and metastasis. Up to now, more than 300 angiogenesis inhibitors have been developed. There are 80 antiangiogenic drugs currently in clinical trials. Notably many inhibitors of angiogenesis have been discovered in natural resources, such as fungi, mushrooms, shark muscle and cartilage, sea coral, green tea, ginseng, and garlic by screening of ECs cultures.¹¹

Received: January 7, 2011

Published: August 19, 2011

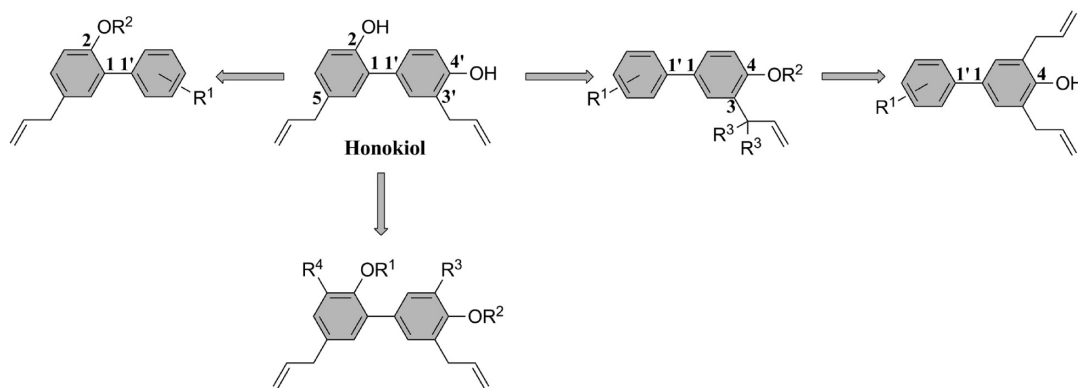
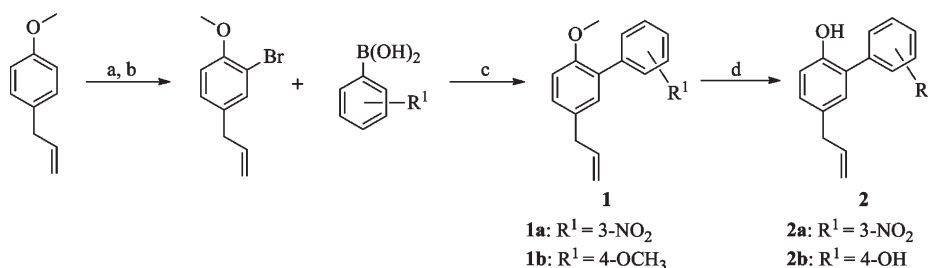


Figure 1. Optimization of building blocks for the synthesis of the biphenolic scaffold.

Scheme 1. Synthesis of Compounds 1, 2a–b^a



^a Reagents and conditions: (a) py·HBr₃, glacial acetic acid; (b) Zn dust, glacial acetic acid; (c) Pd(OAc)₂, PPh₃, K₂CO₃ (2 M), DMF, N₂ atmosphere, 90 °C; (d) BBr₃, -15 °C to room temperature.

Honokiol, a biphenolic neolignan with inappreciable toxicity isolated from *Magnolia officinalis*, has been reported to possess antiangiogenic and antitumor property in several tumor cell lines and tumor xenograft models.^{12,13} However, only a few studies have focused on the structural modification and structure–activity relationship (SAR) of honokiol analogues and derivatives targeting angiogenesis or cancer. Disconnections and chemical synthesis have been undertaken to develop novel honokiol analogues and derivatives to improve biological activity or clarify the SAR.¹⁴ Recent studies in our laboratory were devoted to the structurally modified honokiol with a continuing effort to develop more potent antitumor molecules.^{15,16}

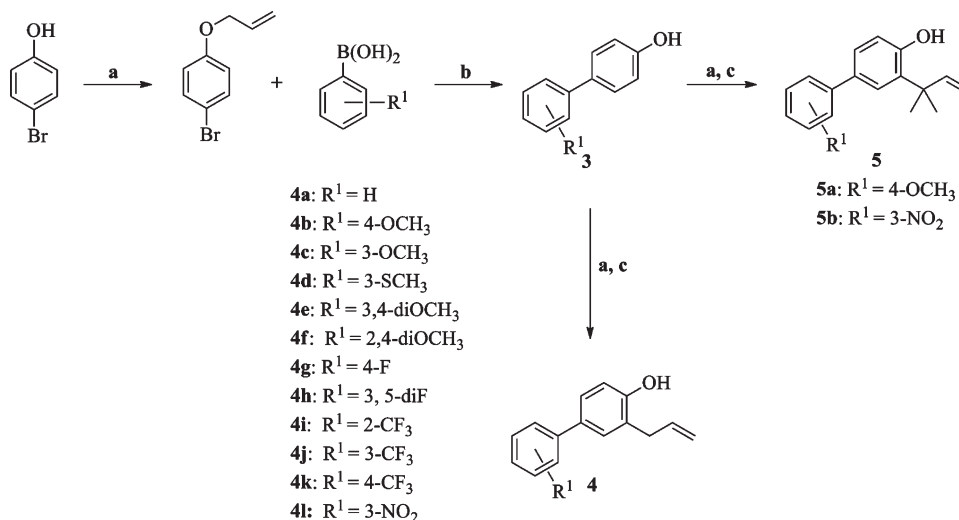
In this study, a series of honokiol analogues and derivatives were designed (Figure 1), synthesized, and subsequently screened. Among them, **8c** effectively suppressed the formation of new blood vessels in zebrafish-based assay and exhibited a medium inhibitory effect on HUVECs (human umbilical vein endothelial cells; IC₅₀ = 15.1 μM) in contrast to honokiol (IC₅₀ = 52.6 μM). Analogue **8c** moderately blocked the proliferation of A549 (human lung carcinoma; IC₅₀ = 30.2 μM), HepG2 (human hepatocellular liver carcinoma; IC₅₀ = 10.7 μM), and LL/2 cells (Lewis lung carcinoma; IC₅₀ = 21.7 μM) superior to honokiol. Importantly, **8c** exerted more potent inhibitory potencies against the migration and tube formation of HUVECs than those of honokiol. The results of *in vivo* antiangiogenic effect and *in vitro* antiproliferative activity of honokiol analogues and derivatives have led to the establishment of a SAR.

Chemistry. 4-Allyl-2-bromoanisole was synthesized from commercially available 4-allylanisole according to the previously reported method¹⁷ and employed 2.8 equiv of pyridinium hydrobromide perbromide (py·HBr₃) followed by further debromination with zinc

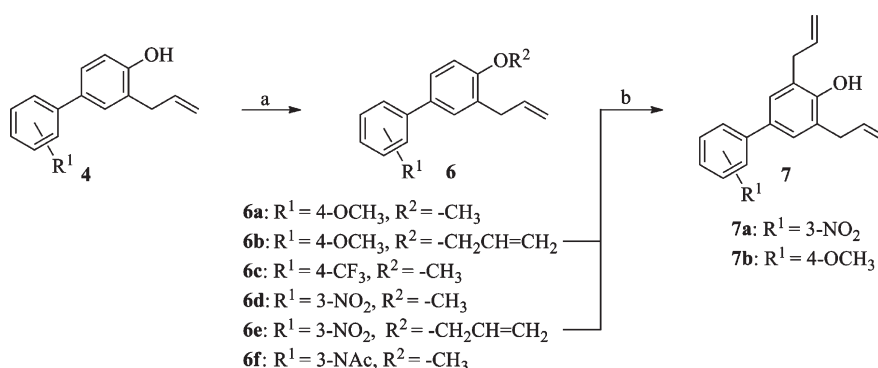
dust (Scheme 1). Suzuki coupling of 4-allyl-2-bromoanisole with appropriate arylboronic acids led to the corresponding 2-*O*-methyl biphenyl derivatives (**1a–b**), which then was demethylated under boron tribromide (BBr₃) to yield 2-phenolic hydroxyl biphenyl derivatives (**2a–b**).

In Scheme 2, the intermediate **3** was prepared through Suzuki cross-coupling reaction. Two cross-coupling methods were developed for condensation of appropriate arylboronic acids with 1-(allyloxy)-4-bromobenzene under palladium catalyst. The *O*-allylation of **3** with 3-bromoprop-1-ene or 1-bromo-3-methylbut-2-ene was performed in the presence of potassium carbonate as base and acetone as solvent, and then derivatives (**4a–l**, and **5a–b**) were synthesized through Claisen rearrangement in *N,N*-diethylaniline as a valid solvent. Moreover, compounds **6a–f** and **7a–b** were obtained by following similar synthetic methods (Scheme 3).

Williamson alkylation of alkyl halide with phenolic hydroxyl groups of honokiol was accomplished by employing potassium carbonate as base, and DMF as solvent. Reimer–Tiemann reaction was performed for the introduction of aldehyde group to the honokiol scaffold using chloroform and sodium hydroxide at 50 °C. In theory, three formylated honokiol analogues should be synthesized, and in fact, only two formylated analogues (i.e., 3-formylated honokiol, **8a**, and 3,5'-diformylated honokiol, **8c**) were obtained because of low ortho-regioselectivity in the Reimer–Tiemann reaction. Because the chemical environment of two phenolic hydroxyl groups of honokiol occurring was similar, highly regioselective Reimer–Tiemann reaction and chemoselective Williamson alkylation were not readily achieved (Scheme 4). Therefore, the crude synthetic samples of analogues were separated by

Scheme 2. Synthesis of Compounds 4a–l and 5a–b^a

^a Reagents and conditions: (a) BrCH₂CH=CH₂ or BrCH₂CH=C(CH₃)₂, K₂CO₃, acetone, reflux, 5 h; (b) method A: Pd(OAc)₂, PPh₃, K₂CO₃ (2 M), isopropyl alcohol, N₂ atmosphere, 90 °C, overnight; method B: Pd(PPh₃)₄, DMF, K₃PO₄·3H₂O (2 M), N₂ atmosphere, 100 °C, overnight; (c) *N,N*-diethylaniline, reflux, overnight.

Scheme 3. Synthesis of Compounds 6a–f, and 7a–b^a

^a Reagents and conditions: (a) CH₃I or BrCH₂CH=CH₂, K₂CO₃, acetone, reflux, overnight; (b) *N,N*-diethylaniline, reflux, overnight.

reversed-phase high-performance liquid chromatography (preparative HPLC) and high-performance counter-current chromatography (HPCCC).¹⁸ At this stage, the products were fully analyzed and characterized by NMR, MS, and HPLC before being submitted to the biological screening.

RESULTS AND DISCUSSION

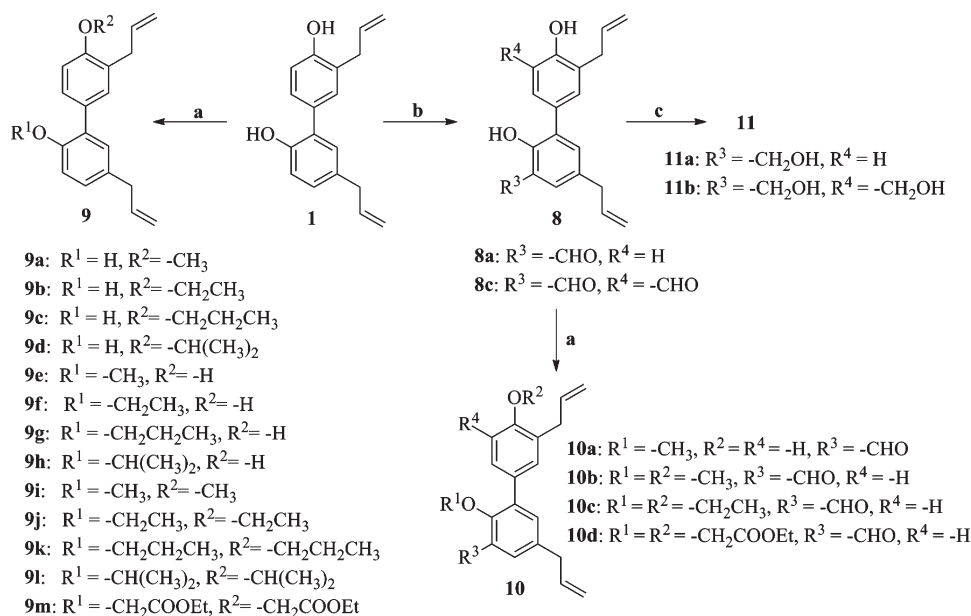
Antiangiogenic Effects in the Transgenic Zebrafish Model.

Recently, zebrafish has been extensively used as an *in vivo* drug screening model for investigating the formation of new blood vessels during the stages of angiogenesis.¹⁹ Zebrafish embryos are transparent and inhibitors or drugs dissolved in dimethylsulfoxide (DMSO) are readily permeable through the chorion. In the present study, all honokiol analogues and derivatives were incubated with the transgenic *fli-1*: enhanced GFP zebrafish embryos that carried a 15-kb *fli-1* promoter which could drive the expression of GFP in the entire endothelium.^{7c}

At a concentration of 10 μM, the antiangiogenic rates of the majority of compounds listed in Table 1 were less than 25%, with

the exception of 8a, 8c, and honokiol. The remaining analogues and derivatives (not listed) were inactive even at concentrations exceeding 40 μM. However, honokiol and 8a were toxic or lethal to zebrafish embryos at a concentration of 40 μM. The antiangiogenic effects of 9a and 10a were moderate at 20 μM and not greatly improved when the concentration reached 40 μM (Figure 2). Importantly, analogue 8c inhibited intersomitic vessel sprouts arising from the dorsal aorta and exhibited the higher antiangiogenic activity in a concentration-dependent manner (Figure 3).

Inspection of their structural features and antiangiogenic activities highlighted that all pharmacologically active analogues and derivatives based on a biphenyl scaffold should possess the 2- and/or 4'-OH group. Introduction of electron-withdrawing groups (EWG; e.g., nitrated in 4l, 5b, and 7a; trifluoromethylated in 4i–k; monofluorinated in 4g; and difluorinated in 4h) and electron-donating groups (EDG; e.g., hydroxylated in 2b; monomethoxylated in 4b–c; dimethoxylated in 4e–f; methylthiolated in 4d; and allylated in 7b) to the biphenyl moiety failed to improve their antiangiogenic potencies in contrast to honokiol.

Scheme 4. Synthesis of Various Analogues from Honokiol Scaffold^a

^a Reagents and conditions: (a) CH₃I; C₂H₅I; CH₃CH₂Br; BrCH₂COOC₂H₅; (CH₃)₂CHI; DMF, K₂CO₃, 30 °C, 6 h; (b) CHCl₃, 35% NaOH (aq), 50 °C, 1 h; (c) methanol, NaBH(OAc)₃, glacial acetic acid, ice bath to room temperature, overnight.

Table 1. Antiangiogenic Effects in Zebrafish Embryos

comps	antiangiogenic effects ^a			
	5 μM	10 μM	20 μM	40 μM
honokiol	+	++	+++	dead ^b
2a	○	+	+	nd ^c
2b	○	+	+	nd
4i	○	+	+	+
4h	+	+	+	+
4k	○	+	+	+
5b	○	○	+	+
7a	○	+	+	+
7b	○	+	+	+
8a	+	++	++	dead
8c	+	++	+++	++++
9a	+	+	++	++
9d	○	+	+	nd
9g	○	+	+	+
9h	+	+	+	+
10a	+	+	++	++
10b	+	+	+	+
10c	○	+	+	+

^a The semiquantitative scale for angiogenic inhibitory rates: ○, inactive; +, < 25% suppression of angiogenesis as compared to the vehicle treated zebrafish embryos. ^b Zebrafish embryos treated with the indicated concentration of compound were dead. ^c Not determined.

The alkylation of the phenolic hydroxyl group of **6**, **9**, and **10** also lowered the inhibitory activity. With respect to these modified analogues based on honokiol, we found that the presence of an aldehyde group at the 3- or/and 5'-position (3-formylated in **8a**,

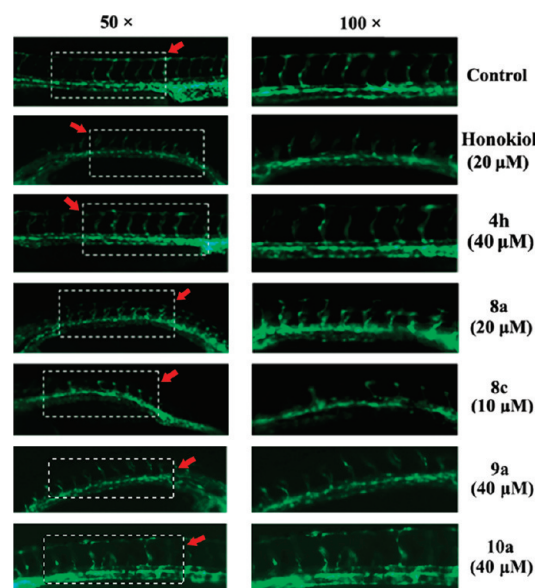


Figure 2. Effects on neovascularization in zebrafish embryos. The transgenic *fli-1*: enhanced GFP zebrafish embryos in embryo water (0.2 g/L of instant ocean salt in distilled water) incubated with the indicated concentrations of compounds at 6 h postfertilization (hpf) for 24 h. Zebrafish embryos were imaged and the number of angiogenic vessels in the trunk was quantified. The left boxed area (red arrowhead) were magnified and shown in the right section (magnification: left, 50×; right, 100×).

and 3,5'-diformylated in **8c**) seemed to be crucial for the antiangiogenic effects.

Antiproliferative Activity and SAR Study. An important strategy for antiangiogenic therapy is effectively inhibiting the proliferation of ECs. Thus, the IC₅₀ value against HUVECs was selected as the main index. Because few analogues and derivatives

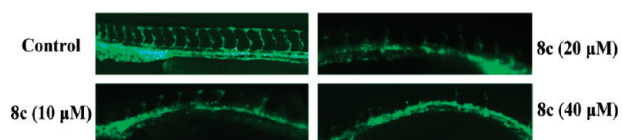


Figure 3. Effects of different concentrations of **8c** on neovascularization in zebrafish embryos. Analogue **8c** concentration-dependently (10, 20, and 40 μM) suppressed the intersomitic vessel sprouts and dorsal longitudinal anastomotic vessels at 6 hpf for 48 h.

were found to possess antiangiogenic potency, we further evaluated their antiproliferative effects on HUVECs and cytotoxic activities against tumor cell lines (A549, HepG2, and LL/2) by 3-[4,5-dimethylthiazol-2-yl]-2,5-diphenyltetrazolium bromide (MTT) assay.

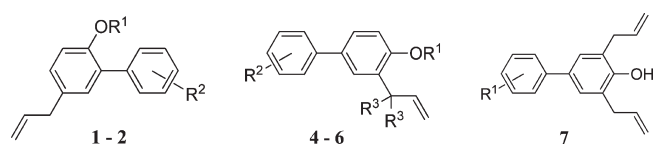
As shown in Table 2, 2-*O*-methyl derivatives (**1a–b**) exhibited no inhibitory activity against the proliferation of HUVECs compared to the corresponding 2-*O*-demethyl derivatives (**2a–b**). Although **2b** bearing a 4'-OH group manifested the higher potency against HUVECs than 3'-nitro derivative **2a**, the antiproliferative activities of **2a** and **2b** were both inferior to that of honokiol. From these results, we could predict that the 2- and 4'-OH group of the biphenyl moiety might be essential for inhibiting the proliferation of HUVECs. Likewise, the number of allyl group potentially affected the cytotoxicity.

Subsequently, we investigated the antiproliferative and cytotoxic activities of the 3-allylbiphenyl-4-ols (**4a–l**, and **5a–b**) and 3-allyl-4-alkoxybiphenyls (**6a–f**). Additionally, 3,5-diallylbiphenyl-4-ols (**7a–b**) were tested for a better understanding of the relationship between the activity and the position and number of the allyl group. In detail, 11 of these derivatives (**4a–c**, **4e–g**, **4l**, **6a–b**, **6d**, and **6e**) were completely inactive against the tested cell lines and all pharmacological profiles were summarized in Table 2. Trifluoromethyl derivatives (2'-CF₃ in **4i**, 3'-CF₃ in **4j**, or 4'-CF₃ in **4k**) exerted less potent antiproliferative activities against HUVECs than honokiol. Although *O*-alkylated derivatives (*O*-methyl in **6c** and *O*-allyl in **6f**) showed weak cytotoxic activities against HepG2 and LL/2 cells, they were unable to suppress the growth of HUVECs. Inspection of their structural features and the activities indicated that lack of the 2-OH and 4-allyl group of the biphenyl scaffold appeared to be unfavorable for the inhibition of HUVECs. Furthermore, 3,5-diallylbiphenyl-4-ols (**7a–b**) also did not achieve the improvement in inhibitory potency in comparison to honokiol which contained 3',5-diallyl groups. The results suggested that the orientation of two allyl groups of the biphenyl scaffold was responsible for the antiproliferative activity. In accordance with in vivo antiangiogenic data from our synthetic derivatives, the introduction of any EDGs or EWGs to the biphenyl scaffold was dispensable for the activity.

The above analysis based on the position of phenolic hydroxyl group and allyl group of the biphenyl scaffold was summarized. Unexpectedly, all aforementioned derivatives showed less potent antiproliferative activities against HUVECs than honokiol. The retention of any reactive functional groups (phenolic hydroxyl group or allyl group) of the biphenyl scaffold has been proven to be required for the inhibitory potency. Consequently, our synthetic strategy was further devoted to keep the honokiol moiety intact.

As shown in Table 3, if the 2-phenolic hydroxyl group of honokiol was alkylated, the antiproliferative effect on HUVECs decreased with the increase of alkyl chain length (methyl in **9a**; ethyl in **9b**; propyl in **9c**; and isopropyl in **9d**) compared to that

Table 2. IC₅₀ Values of Derivative (1–2 and 4–7) against HUVECs, A549, HepG2, and LL/2 Cell Lines

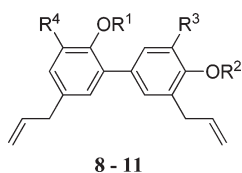


compd	IC ₅₀ (μM)			
	HUVECs	A549	HepG2	LL/2
honokiol	52.6	35.0 ^a	16.5 ^b	65.4
1a	>100.0	>100.0	>100.0	89.4
1b	>100.0	95.4	>100.0	71.1
2a	79.1	>100.0	62.3	61.4
2b	64.3	76.2	89.0	>100
4a	>100.0	>100.0	>100.0	>100.0
4b	>100.0	>100.0	>100.0	>100.0
4c	>100.0	>100.0	>100.0	>100.0
4d	>100.0	66.0	>100.0	>100.0
4e	>100.0	>100.0	>100.0	>100.0
4f	>100.0	>100.0	>100.0	>100.0
4g	>100.0	>100.0	>100.0	>100.0
4h	80.0	>100.0	>100.0	78.2
4i	82.0	59.7	52.4	60.3
4j	76.0	73.0	58.3	65.9
4k	74.0	76.0	60.3	74.8
4l	>100.0	>100.0	>100.0	>100.0
5a	>100.0	>100.0	91.0	>100.0
5b	77.0	64.0	56.0	45.1
6a	>100.0	>100.0	>100.0	>100.0
6b	>100.0	>100.0	>100.0	>100.0
6c	>100.0	>100.0	89.0	78.8
6d	>100.0	>100.0	>100.0	>100.0
6e	>100.0	>100.0	>100.0	>100.0
6f	>100.0	>100.0	60.1	65.1
7a	>100.0	80.0	80.5	56.5
7b	>100.0	75.6	69.2	60.3

^aData was cited from ref 13. ^bData was cited from ref 14e.

of honokiol, suggesting that the free 2-phenolic hydroxyl group potentially affected the antiproliferative activity and that the alkylation of honokiol was detrimental to the activity. This consistent tendency also occurred in 4'-*O*-alkyl analogues (**9e–f**), and yet their inhibitory potencies were less strong than those of analogues **9a–d**, stating that the contribution of 2-OH group was slightly superior to the 4'-OH of honokiol. When both the phenolic hydroxyl groups of honokiol were alkylated, the corresponding analogues (**9i–m**) were almost inactive against the proliferation of HUVECs, indicating that the number of the bare phenolic hydroxyl group contributed to antiproliferation.

To our surprise, the introduction of the aldehyde group at 3- and/or 5'-position of honokiol exhibited a remarkable enhancement of antiproliferative effect on HUVECs and cytotoxicity against tumor cells (Table 3). Analogue **8c** (IC₅₀ = 15.1 μM) achieved 3.5- and 3.0-fold improvements in the inhibition of HUVECs compared to honokiol (IC₅₀ = 52.6 μM) and **8a** (IC₅₀ = 46.2 μM). Meanwhile, **8c** moderately suppressed the growth of A549, HepG2, and LL/2

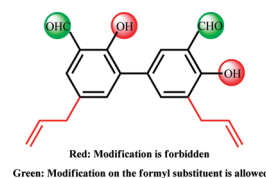
Table 3. IC₅₀ Values of Honokiol Analogues (8–11) against HUVECs, A549, HepG2, and LL/2

compd	IC ₅₀ (μM)			
	HUVECs	A549	HepG2	LL/2
8a ^a	46.2	43.6	32.9	65.3
8c	15.1	30.2	10.7	21.7
9a	55.8	nd ^b	55.3	68.8
9b	67.1	51.0	73.8	61.6
9c	89.3	82.4	>129.9	64.8
9d	70.5	42.7	48.4	49.1
9e	61.8	nd	57.5	108.3
9f	68.2	81.6	71.5	67.6
9g	73.3	53.8	49.9	45.8
9h	65.5	53.2	63.5	48.4
9i	>100.0	nd	>135.98	>136.00
9j	>100.0	>124.2	>124.2	>124.2
9k	>100.0	>114.2	>114.2	>114.2
9l	>100.0	>114.2	>114.2	>114.2
9m	>100.0	>91.3	68.9	>91.3
10a	32.5	28.6	20.9	20.4
10b	39.1	42.6	53.9	40.8
10c	37.9	39.0	28.5	31.9
10d	86.9	>85.8	>85.2	26.1
11a	>100.0	>135.0	>135.0	>135.0
11b	>100.0	>122.6	>122.6	>122.6

^aData was cited from ref 16. ^bNot determined.

tumor cells, with the IC₅₀ values of 30.2, 10.7, and 21.7 μM, respectively. The *O*-alkylation of **8a** led to four corresponding analogues (**10a–d**), and their antiproliferative potencies against HUVECs in comparison to those of **8c** were not notably improved. As a consequence, we could surmise that the phenolic hydroxyl groups of honokiol play critical roles in the inhibitory activity. Chemical reduction of the aldehyde group of **8a** and **8c** rendered their counterparts (**11a** and **11b**) inactive, highlighting that the reactive aldehyde group was profitable to the activity.

Overall, a SAR of honokiol analogues and derivatives (Figure 4) has been summarized as follows: (a) All the biologically active honokiol analogues and derivatives possessed the 2- and/or 4'-OH of the biphenyl scaffold. As for the position of phenolic hydroxyl groups of honokiol, the C-2 site was slightly superior to the C-4' site (e.g., **9a** vs **9e**). The *O*-alkylation inevitably reduced the activity (e.g., **9i** vs honokiol). (b) The introduction of the aldehyde group at the 3- and/or 5'-position of honokiol has been approved to be critical for antiangiogenic and antiproliferative activity (e.g., **8c** vs. honokiol). A similar study has been reported that the formylated compound exerted a favorable inhibitory effect on the migration and invasion of HT1080 cells.²⁰ (c) The introduction of any EWGs or EDGs did not achieve major improvements in the inhibitory potency (e.g., **4i** vs. honokiol). (d) The position and number of the allyl groups of honokiol should be forbidden to

**Figure 4.** Structure–activity relationships of honokiol analogues and derivatives.

change. If the position and number were modified, the corresponding compounds become inactive (e.g., **7b** vs. honokiol).

Honokiol is also a potent antiviral,^{14a,b} neurotrophic,^{14c} and antioxidative agent.^{14d} The antiproliferative SAR of honokiol analogues and derivatives was similar to ones of the previous reports with the difference occurring in the structural modification of the aldehyde group at the 3- and/or 5'-position (Figure 4).¹⁴ The introduction of two aldehyde groups to honokiol achieved improvements in the *in vivo* antiangiogenic potency and *in vitro* antiproliferative activity against the four cell lines. The aforementioned results validated that honokiol as a drug-like lead was extremely promising.

Effects on the HUVECs Migration. The migration of ECs is an important process of chemotaxis and an indispensable step to generate new blood vessels. Inhibition on this process will block the formation of new blood vessels. Therefore, wound-healing migration assay was applied to assess the HUVECs migration. With comparable or superior to honokiol in antiangiogenic and antiproliferative activity, analogues **8a**, **8c**, **9a**, and **10a** were next selected for biological evaluation. As illustrated in Figure 5, the HUVECs actively migrated into the wound area (between the two white lines) under the compound-free condition (control). At a concentration of 20 μM, analogues **8a** and **8c** manifested nearly equal potency to that of honokiol, and stronger inhibition than those of **9a** and **10a**. While the tested compounds' concentration reached 40 μM, the HUVECs migratory rates of **8a**, **8c**, **9a**, **10a**, and honokiol were 34.2, 21.2, 54.2, 63.2, and 38.5%, respectively. Analogue **8c** statistically exerted the higher potent inhibitory effect on the migration of HUVECs, reaching a 1.5-fold improvement over honokiol.

Effects on the HUVECs Tube Formation. In the later stages of angiogenesis, ECs will assemble into an interconnected tubular network which is nearly identical to *in vivo* capillary vascular beds. Inhibition on the formation of capillary-like tube networks will terminate the development of new blood vessels. Thus, a tube formation assay by plating HUVECs on Matrigel was performed. In the control, cells showed the high mobility on Matrigel and formed an intact tubular network in 12 h (Figure 6I). In comparison with the control group, the inhibitory rates of tube formation treated with **8a**, **8c**, **9a**, **10a**, and honokiol at a concentration of 20 μM were 41.2, 21.3, 34.9, 82.5, and 51.4%, respectively (Figure 6II). Our observation indicated that **8c** approximately achieved a 2.5-fold improvement in the inhibition of tube formation compared to that of honokiol at the same concentration and the intact tubular structures disrupted by 20 μM **8c** were sparse and incomplete.

CONCLUSION

The strategy of antiangiogenic therapy provides an alternative that uses the evolving vessels, which nourishes the growth and metastasis of tumor, as the attractive and prime target.²¹ The ECs activation, proliferation, invasion, migration, and tube formation are the fundamental steps for angiogenesis. However, acquired

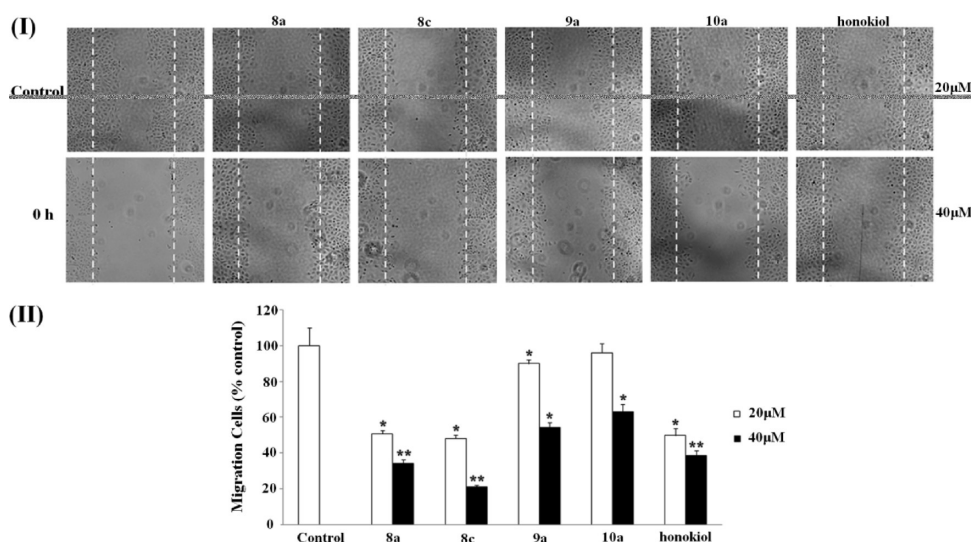


Figure 5. Effects on the HUVECs migration. (I) HUVECs suspended in serum-free Dulbecco's Modified Eagle Medium (DMEM) containing compounds (20 or 40 μM) for 24 h were photographed under a phase contrast microscopy (magnification: 50 \times). Control was treated with serum-free DMEM. (II) Inhibitory rates of compounds on the HUVECs migration. Data represented the mean \pm standard error (SE) from three independent experiments. * $P < 0.05$; ** $P < 0.01$.

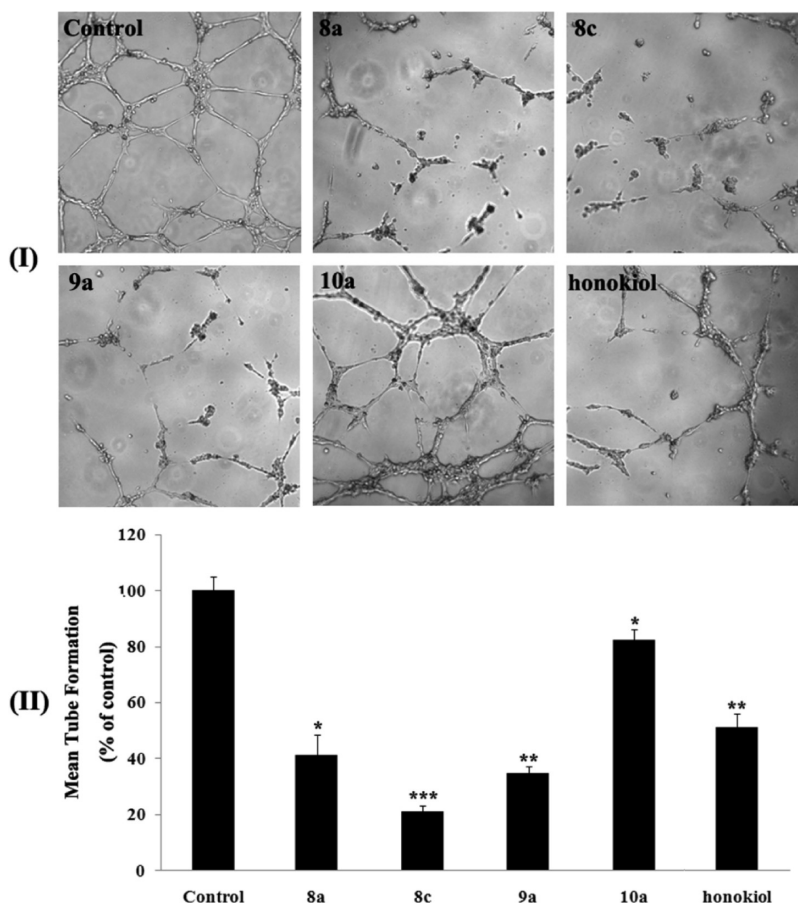


Figure 6. Effects on the HUVECs tube formation. (I) HUVECs (1×10^4 cells) suspended in DMEM containing each compound (20 μM) were added to the Matrigel. Control was treated with DMEM alone. After incubation for 12 h at 37 $^{\circ}\text{C}$, capillary networks were photographed and quantified (magnification: 100 \times). (II) Inhibitory rates of compounds on the HUVECs tube formation. The number of intact tubes was counted in five randomly chosen regions and expressed as the percentage of the control. The results were expressed as mean \pm SE * $P < 0.05$; ** $P < 0.01$; *** $P < 0.005$.

drug resistance remains a major obstacle of tumor targeting therapy.²² In comparison with genetically unstable tumor cells, the ECs recruited by new tumor vasculatures are genetically more stable and less susceptible to acquired drug resistance.²³ Therefore, blocking angiogenesis, specifically targeting ECs, has been proven to be a feasible strategy for preventing angiogenesis-dependent tumor growth and metastasis.

Herein, 47 honokiol analogues and derivatives represented an allylated biphenolic scaffold and possessed a unique mode of action in antiangiogenic and antitumor activity. In detail, **8c** moderately blocked the newly grown segmental vessels from the dorsal aorta in the transgenic zebrafish-based assay, exhibited the strongest inhibitory effects on the proliferation, migration, and tube formation of HUVECs featuring antiangiogenic property in this study, and also exerted its medium cytotoxicity against the selected tumor cell lines (A549, HepG2, and LL/2). Additionally, the further mechanism of antiangiogenesis (e.g., targeting vascular endothelial growth factor (VEGF) or fibroblast growth factor (FGF)), *in vivo* antitumor evaluation, and structural modification of **8c** are in progress.

EXPERIMENTAL SECTION

Cell Culture. HUVECs were isolated from human umbilical cord with collagens. After dissociation, the cells were collected and cultured on gelatin-coated culture flasks in M-199 medium with 20% fetal bovine serum (FBS), 10 ng/mL basic FGF, 2 ng/mL VEGF, 100 IU/mL penicillin, and 100 µg/mL streptomycin. Subcultures were performed with trypsin–ethylene diamine tetraacetic acid (EDTA). Media were refreshed every two days. HUVECs were confirmed by their cobblestone morphology and strong positive immunoreactivity to von Willebrand factor. All cells were incubated in an atmosphere containing 5% CO₂ at 37 °C.

MTT Assay. MTT assay was performed to evaluate the cytotoxic and antiproliferative activities of all compounds. Cells were treated with various concentrations of compound in 96-well culture plates for 24 h in final volumes of 200 µL (5×10^3 cells/well). Then 20 µL of MTT solution (5 mg/mL) was added to each well, and cells were incubated for an additional 3 h. Then the medium was carefully removed, and precipitates were dissolved in 150 µL of DMSO, shaken mechanically for 30 min, and then absorbance values at a wavelength of 570 nm were taken on a spectrophotometer (Molecular Devices, Sunnyvale, USA). IC₅₀ values were calculated using percentage of growth versus untreated control.

Wound-Healing Assay. HUVECs were seeded in 6-well plates precoated with 0.1% gelatin and grown overnight to confluence. The monolayer cells were wounded by scratching with 10 µL pipet tips and washed twice with serum-free DMEM to remove the nonadherent cells and then replaced by serum-free DMEM with the indicated concentrations of compounds for 24 h. Images were taken at 0 h and 24 h independently after incubation at 37 °C, 5% CO₂. The migrated HUVECs were manually counted. The values were observed from three randomly selected fields. Similar patterns of the inhibition were observed in three independent experiments.

Tube Formation Assay. Matrigel was dissolved at 4 °C overnight. Each well of prechilled 96-well plates was coated with 50 µL of Matrigel, incubated and solidified at 37 °C for 45 min. After removing the unsolidified fluid, HUVECs at the density of 1×10^4 were cultured in DMEM containing the indicated concentrations of compounds for 24 h. Controls are treated with the DMEM alone. Images were digitally captured and quantitatively analyzed (Olympus).

Zebrafish Embryos Assay. Using transgenic *fli-1*: enhanced GFP zebrafish embryos, we examined the effects of all compounds on embryonic

angiogenesis. Zebrafish embryos were generated by natural pairwise mating and raised at 28.5 °C in embryo water (0.2 g/L of Instant Ocean Salt in distilled water). At about 6 hpf, the embryos were sorted in the 6-well plate (6 embryos/well), removing dead and unhealthy embryos. Then the embryos were treated with the indicated concentrations of compounds which were added into embryo water. After incubation for 24 or 48 h, the embryos were anesthetized using 0.05% 2-phenoxyethanol in embryo water, photographed, and quantified.

Chemistry. NMR spectra were recorded at 400 MHz on a Varian spectrometer (Varian, Palo Alto, CA, USA) model Gemini 400 and reported in parts per million. Chemical shifts (δ) are quoted in ppm relative to tetramethylsilane (TMS) as an internal standard, where (δ) TMS = 0.00 ppm. The multiplicity of the signal is indicated as s, singlet; d, doublet; t, triplet; q, quartet; m, multiplet, defined as all multiplet signals where overlap or complex coupling of signals makes definitive descriptions of peaks difficult. MS spectra were measured by quadrupole-time-of-flight (Q-TOF) Premier mass spectrometer utilizing electrospray ionization (ESI) (Micromass, Manchester, UK). Room temperature is within 20–25 °C. The purity of compound was determined to be $\geq 97\%$ by HPLC analysis (Supporting Information). The synthetic methods of **1a–b** and **2a–b** were referred from the reported literature.¹⁷ The structural elucidations of **8a**, **8c**, **10a**, and **10b** have been reported in our previous literatures.¹⁸

5-Allyl-2-methoxy-3'-nitro-1,1'-biphenyl (1a). Yield 87.0%. ¹H NMR (400 MHz, CDCl₃): δ 8.58 (t, 1H, *J* = 2.0 Hz, 2'-H), 8.22–8.18 (m, 1H, 4'-H), 7.92–7.78 (m, 2H, 5'- and 6'-H), 7.68–7.53 (m, 2H, 4- and 6-H), 6.93–6.91 (m, 1H, 3-H), 6.19–6.11 (m, 1H, $-\text{CH}=\text{CH}_2$), 5.34–5.30 (m, 2H, $-\text{CH}=\text{CH}_2$), 3.83 (s, 3H, $-\text{OCH}_3$), 3.49 (d, 2H, *J* = 5.4 Hz, $-\text{CH}_2\text{CH}$). HRMS [*M* + *H*]⁺ calcd 270.1130; found 270.1122.

5-Allyl-2,4'-dimethoxy-1,1'-biphenyl (1b). Yield 65.7%. ¹H NMR (400 MHz, CDCl₃): δ 7.69–7.61 (m, 2H, 2'- and 6'-H), 7.23–7.18 (m, 2H, 3'- and 4'-H), 7.07–7.01 (m, 1H, 6-H), 6.98–6.96 (m, 2H, 3- and 4-H), 6.12–6.05 (m, 1H, $-\text{CH}=\text{CH}_2$), 5.31–5.29 (m, 2H, $-\text{CH}=\text{CH}_2$), 3.89 (s, 3H, 4'-OCH₃), 3.85 (s, 3H, 2-OCH₃), 3.49 (d, 2H, *J* = 5.2 Hz, $-\text{CH}_2\text{CH}$). HRMS [*M* + *H*]⁺ calcd 255.1385; found 255.1401.

5-Allyl-3'-nitro-[1,1'-biphenyl]-2-ol (2a). Yield 71.3%. ¹H NMR (400 MHz, CDCl₃): δ 8.60 (s, 1H, 2'-H), 8.20–8.18 (m, 1H, 4'-H), 7.91–7.89 (m, 1H, 6'-H), 7.65–7.57 (m, 2H, 5'- and 6-H), 6.96–6.91 (m, 2H, 3- and 4-H), 6.22–6.18 (m, 1H, $-\text{CH}=\text{CH}_2$), 5.58 (s, 1H, $-\text{OH}$), 5.32–5.28 (m, 2H, $-\text{CH}=\text{CH}_2$), 3.49 (d, 2H, *J* = 5.4 Hz, $-\text{CH}_2\text{CH}$). HRMS [*M* – *H*][–] calcd 254.0817; found 254.0814.

5-Allyl-[1,1'-biphenyl]-2,4'-diol (2b). Yield 54.9%. ¹H NMR (400 MHz, CDCl₃): δ 7.62–7.58 (m, 3H, Ar-H), 7.33–7.30 (m, 1H, Ar-H), 6.96–6.94 (m, 3H, Ar-H), 6.10–6.03 (m, 1H, $-\text{CH}=\text{CH}_2$), 5.31–5.29 (m, 2H, $-\text{CH}=\text{CH}_2$), 3.48 (d, 2H, *J* = 5.4 Hz, $-\text{CH}_2\text{CH}$). HRMS [*M* – *H*][–] calcd 225.0916; found 225.0899.

Typical Procedure for the Synthesis of 4a–l, and 5a–b. *Step I: Synthesis of 1-Allyloxy-4-bromobenzene.* To a mixture of 4-bromophenol (3.5 g, 20.0 mmol) and anhydrous potassium carbonate (3.6 g, 26.0 mmol, 1.3 equiv) in acetone (25 mL), allyl bromide (1.9 mL, 22.0 mmol, 1.1 equiv) was added dropwise. The mixture was heated at 60 °C for 5 h. After cooling, the mixture was filtered and the solution was evaporated to dryness. Then the filtrate was extracted with diethyl ether (20 mL \times 3) and 10% NaOH (20 mL \times 1) and the organic layer was washed by brine (20 mL \times 2), dried over anhydrous magnesium sulfate, and concentrated under reduced pressure to afford a colorless oil product (4.1 g, 19.0 mmol, 95.0%).

Step II: Synthesis of Intermediates 3 by Suzuki-Coupling Reaction. Method A (for 4a–f). 1-Allyloxy-4-bromobenzene (1.0 mmol) and arylboronic acid (1.2 mmol) were dissolved in isopropyl alcohol (4 mL) at room temperature. After becoming a clear solution, Pd(OAc)₂ (0.01 mmol), PPh₃ (0.03 mmol), and a solution of anhydrous potassium carbonate (2.0 mmol) in water (1 mL) were added at N₂ atmosphere, and the resulting mixture was stirred for further 18 h at 90 °C. The mixture was filtered and extracted with ethyl acetate (3 \times 10 mL).

The extract was washed by brine (2 × 10 mL), dried over anhydrous sodium sulfate, and concentrated. The residue was purified by gel chromatography (ethyl acetate:petroleum ether = 1:10) to give our target compound with a satisfactory yield.

Method B (for 4g–l). 1-Allyloxy-4-bromobenzene (1.0 mmol) and arylboronic acid (1.2 mmol) were dissolved in DMF (4 mL) at room temperature. After becoming a clear solution, Pd(PPh₃)₄ (0.01 mmol) and a solution of K₃PO₄ · 3H₂O (2.0 mmol) in water (1 mL) were added at N₂ atmosphere, and the mixture was stirred for further 18 h at 100 °C (TLC monitoring). The mixture was filtered and extracted with ethyl acetate (3 × 10 mL). The extract was washed by brine (2 × 10 mL), dried over anhydrous sodium sulfate, and concentrated. The residue was further purified by gel chromatography (ethyl acetate:petroleum ether = 1:10) to give our target compound.

Step III: Synthesis of 4a–l and 5a–b. Allyl bromide or 1-bromo-3-methylbut-2-ene (1.3 mmol) was added to the solution of 3 (1.0 mmol) and anhydrous potassium carbonate (2.0 mmol) and refluxed for 5 h (TLC monitoring). After cooling, the mixture was filtered and the solution was evaporated to dryness. Then the crude was extracted by diethyl ether (2 × 10 mL), and the organic layer was washed by brine (2 × 10 mL), dried over anhydrous sodium sulfate, and concentrated under reduced pressure to afford the product. And then the product was dissolved in *N,N*-diethylaniline and refluxed overnight, monitored by thin-layer chromatography (TLC). After reaction was completed, the solution was adjusted to pH = 4 by 3N HCl and extracted with ethyl acetate (2 × 10 mL) and the organic layer was washed by water and brine, dried over anhydrous magnesium sulfate, and concentrated under reduced pressure to afford the crude product. The residue was further purified by silica gel column chromatography (ethyl acetate:petroleum ether = 1:10) to give our target compounds. The yield was depicted as the total yield of four steps.

3-Allyl-[1,1'-biphenyl]-4-ol (4a). Yield 32.8%. ¹H NMR (400 MHz, CDCl₃): δ 7.55–7.53 (m, 2H, 2- and 6-H), 7.43–7.36 (m, 4H, Ar'-H), 7.32–7.28 (m, 1H, 4'-H), 6.89 (d, 1H, J = 8.4 Hz, 5-H), 6.11–6.01 (m, 1H, -CH=CH₂), 5.24–5.18 (m, 2H, -CH=CH₂), 4.98 (br s, 1H, -OH), 3.48 (d, 2H, J = 5.4 Hz, -CH₂CH). HRMS [M + Na]⁺ calcd 233.0942; found 233.0939.

3-Allyl-4'-methoxy-[1,1'-biphenyl]-4-ol (4b). Yield 58.9%. ¹H NMR (400 MHz, CDCl₃): δ 7.48–7.46 (m, 2H, 2'- and 6'-H), 7.33–7.30 (m, 2H, 2- and 6-H), 6.96–6.94 (m, 2H, 3'- and 4'-H), 6.86 (d, 1H, J = 8.4 Hz, 5-H), 6.11–6.01 (m, 1H, -CH=CH₂), 5.23–5.17 (m, 2H, -CH=CH₂), 3.84 (s, 3H, 4-OCH₃), 3.47 (d, 2H, J = 5.4 Hz, -CH₂CH). RMS [M + Na]⁺ calcd 263.1048; found 263.1056.

3-Allyl-3'-methoxy-[1,1'-biphenyl]-4-ol (4c). Yield 51.9%. ¹H NMR (400 MHz, CDCl₃): δ 7.39–7.32 (m, 3H, Ar-H), 7.15 (d, 1H, J = 7.6 Hz, 6-H), 7.09 (s, 1H, 2'-H), 6.90–6.85 (m, 2H, 4'- and 5-H), 6.08–6.04 (m, 1H, -CH=CH₂), 5.24–5.18 (m, 2H, -CH=CH₂), 3.87 (s, 3H, 3-OCH₃), 3.49 (d, 2H, J = 6.4 Hz, -CH₂CH). HRMS [M + H]⁺ calcd 241.1229; found 241.1225.

3-Allyl-3'-(methylthio)-[1,1'-biphenyl]-4-ol (4d). Yield 76.9%. ¹H NMR (400 MHz, CDCl₃): δ 7.42 (s, 1H, 2-H), 7.37–7.29 (m, 4H, Ar-H), 7.21–7.18 (m, 1H, 2'-H), 6.89 (d, 1H, J = 8.4 Hz, 5-H), 6.11–6.01 (m, 1H, -CH=CH₂), 5.24–5.18 (m, 2H, -CH=CH₂), 3.48 (d, 2H, J = 6.4 Hz, -CH₂CH), 2.53 (s, 3H, 3-SCH₃). HRMS [M + H]⁺ calcd 257.1000; found 257.1002.

3-Allyl-3',4'-dimethoxy-[1,1'-biphenyl]-4-ol (4e). Yield 65.9%. ¹H NMR (400 MHz, CDCl₃): δ 7.34–7.30 (m, 2H, 2- and 6-H), 7.09–7.05 (m, 2H, 2'- and 6'-H), 6.93–6.88 (m, 2H, 5- and 5'-H), 6.12–6.02 (m, 1H, -CH=CH₂), 5.23–5.17 (m, 2H, -CH=CH₂), 3.95 (s, 3H, 4-OCH₃), 3.91 (s, 3H, 3-OCH₃), 3.48 (d, 2H, J = 5.4 Hz, -CH₂CH). HRMS [M + H]⁺ calcd 271.1334; found 271.1343.

3-Allyl-2',4'-dimethoxy-[1,1'-biphenyl]-4-ol (4f). Yield 55.9%. ¹H NMR (400 MHz, CDCl₃): δ 7.28–7.19 (m, 3H, 2-, 6-, and 6'-H), 6.82

(d, 1H, J = 8.0 Hz, 5-H), 6.56–6.53 (m, 2H, 3'- and 5'-H), 6.08–6.00 (m, 1H, -CH=CH₂), 5.23–5.14 (m, 2H, -CH=CH₂), 5.11 (s, 1H, -OH), 3.84 (s, 3H, 4-OCH₃), 3.78 (s, 3H, 3-OCH₃), 3.44 (d, 2H, J = 6.4 Hz, -CH₂CH). HRMS [M + Na]⁺ calcd 293.1154; found 293.1150.

3-Allyl-4'-fluoro-[1,1'-biphenyl]-4-ol (4g). Yield 23.9%. ¹H NMR (400 MHz, CDCl₃): δ 7.50–7.46 (m, 2H, 2- and 6-H), 7.32–7.30 (m, 2H, 2'- and 6'-H), 7.11–7.07 (m, 2H, 3'- and 5'-H), 6.88 (d, 1H, J = 8.4 Hz, 5-H), 6.11–6.00 (m, 1H, -CH=CH₂), 5.23–5.18 (m, 2H, -CH=CH₂), 5.05 (s, 1H, -OH), 3.47 (d, 2H, J = 4.8 Hz, -CH₂CH). HRMS [M + H]⁺ calcd 229.1029; found 229.0982.

3-Allyl-3',5'-difluoro-[1,1'-biphenyl]-4-ol (4h). Yield 34.8%. ¹H NMR (400 MHz, CDCl₃): δ 7.35–7.31 (m, 2H, 2- and 6-H), 7.08–7.03 (m, 2H, 2'- and 6'-H), 6.89 (d, 1H, J = 8.0 Hz, 5-H), 6.76–6.69 (m, 1H, 4'-H), 6.10–5.97 (m, 1H, -CH=CH₂), 5.24–5.18 (m, 2H, -CH=CH₂), 5.07 (s, 1H, -OH), 3.48 (d, 2H, J = 6.0 Hz, -CH₂CH). HRMS [M + H]⁺ calcd 269.0754; found 269.0752.

3-Allyl-2'-(trifluoromethyl)-[1,1'-biphenyl]-4-ol (4i). Yield 43.0%. ¹H NMR (400 MHz, CDCl₃): δ 7.72 (d, 1H, J = 7.2 Hz, 6'-H), 7.53 (t, 1H, J = 7.2 Hz, 3'-H), 7.43 (t, 1H, J = 7.2 Hz, 5'-H), 7.32 (d, 1H, J = 7.2 Hz, 4'-H), 7.10–7.08 (m, 2H, 2- and 6-H), 6.84 (d, 1H, J = 8.0 Hz, 5-H), 6.09–5.99 (m, 1H, -CH=CH₂), 5.19–5.15 (m, 2H, -CH=CH₂), 3.44 (d, 2H, J = 6.0 Hz, -CH₂CH). HRMS [M - H]⁻ calcd 277.0840; found 277.0840.

3-Allyl-3'-(trifluoromethyl)-[1,1'-biphenyl]-4-ol (4j). Yield 59.8%. ¹H NMR (400 MHz, CDCl₃): δ 7.77 (s, 1H, 2'-H), 7.72–7.70 (m, 1H, 6'-H), 7.56–7.49 (m, 2H, 2- and 6-H), 7.39–7.35 (m, 2H, 3'- and 4'-H), 6.91 (d, 1H, J = 8.0 Hz, 5-H), 6.11–6.01 (m, 1H, -CH=CH₂), 5.24–5.19 (m, 2H, -CH=CH₂), 3.49 (d, 2H, J = 6.4 Hz, -CH₂CH). HRMS [M + H]⁺ calcd 301.0816; found 301.0820.

3-Allyl-4'-(trifluoromethyl)-[1,1'-biphenyl]-4-ol (4k). Yield 51.8%. ¹H NMR (400 MHz, CDCl₃): δ 7.67–7.62 (m, 4H, Ar'-H), 7.40–7.36 (m, 2H, 2- and 6-H), 6.92 (d, 1H, J = 8.0 Hz, 5-H), 6.10–6.01 (m, 1H, -CH=CH₂), 5.24–5.19 (m, 2H, -CH=CH₂), 3.49 (d, 2H, J = 6.0 Hz, -CH₂CH). HRMS [M + H]⁺ calcd 279.0997; found 279.0897.

3-Allyl-3'-nitro-[1,1'-biphenyl]-4-ol (4l). Yield 81.0%. ¹H NMR (400 MHz, CDCl₃): δ 8.41 (t, 1H, J = 2.0 Hz, 2'-H), 8.16–8.14 (m, 1H, 4'-H), 7.88–7.86 (m, 1H, 6'-H), 7.57 (t, 2H, J = 8.4 Hz, 5'-H), 7.43–7.39 (m, 2H, 2- and 6-H), 6.94 (d, 1H, J = 8.0 Hz, 5-H), 6.12–6.02 (m, 1H, -CH=CH₂), 5.25–5.20 (m, 2H, -CH=CH₂), 3.51 (d, 2H, J = 5.4 Hz, -CH₂CH). HRMS [M + H]⁺ calcd 278.0793; found 278.0785.

4'-Methoxy-3-(2-methylbut-3-en-2-yl)-[1,1'-biphenyl]-4-ol (5a). Yield 22.0%. ¹H NMR (400 MHz, CDCl₃): δ 7.48 (m, 2H, J = 8.4 Hz, 2'- and 6'-H), 7.32–7.28 (m, 2H, 2- and 6-H), 6.96 (d, 2H, J = 8.8 Hz, 3'- and 5'-H), 6.85 (d, 1H, J = 8.8 Hz, 5-H), 5.50 (s, 1H, -OH), 5.12 (s, 1H, -CH=CH₂), 5.06 (s, 1H, -CH=CH₂), 3.84 (s, 3H, 4-OCH₃), 3.62 (d, 1H, J = 7.2 Hz, -CH₂CH), 1.70 (s, 3H, -CH₃), 1.17 (d, 3H, J = 6.8 Hz, -CH₃). HRMS [M + H]⁺ calcd 269.1542; found 269.1539.

3-(2-Methylbut-3-en-2-yl)-3'-nitro-[1,1'-biphenyl]-4-ol (5b). Yield 58.0%. ¹H NMR (400 MHz, CDCl₃): δ 8.40 (s, 1H, 2'-H), 8.15–8.13 (m, 1H, 4'-H), 7.87 (d, 1H, J = 7.6 Hz, 6'-H), 7.57 (t, 1H, J = 8.0 Hz, 5'-H), 7.41–7.38 (m, 2H, 2- and 6-H), 6.94 (d, 1H, J = 8.0 Hz, 5-H), 5.13 (s, 1H, -CH=CH₂), 5.09 (s, 1H, -CH=CH₂), 3.71 (q, 1H, J = 7.2 Hz, -CH₂CH), 1.73 (s, 3H, -CH₃), 1.49 (d, 3H, J = 6.8 Hz, -CH₃). HRMS [M + H]⁺ calcd 284.1287; found 284.1289.

Synthesis of 6a–f: Following Step I of Typical Procedure for the Synthesis of 4a–l. **3-Allyl-4,4'-dimethoxy-1,1'-biphenyl (6a).** Yield 89.5%. ¹H NMR (400 MHz, CDCl₃): δ 7.48 (d, 2H, J = 8.4 Hz, 2'- and 6'-H), 7.38–7.34 (m, 2H, 2- and 6-H), 6.95 (d, 2H, J = 8.4 Hz, 3'- and 5'-H), 6.91 (d, 1H, J = 8.4 Hz, 5-H), 6.07–6.00 (m, 1H, -CH=CH₂), 5.12–5.05 (m, 2H, -CH=CH₂), 3.86 (s, 3H, 4-OCH₃), 3.84 (s, 3H, 4'-OCH₃), 3.44 (d, 2H, J = 6.4 Hz, -CH₂CH). HRMS [M + Na]⁺ calcd 277.1204; found 277.1191.

3-Allyl-4-(allyloxy)-4'-methoxy-1,1'-biphenyl (6b). Yield 95.9%. ¹H NMR (400 MHz, CDCl₃): δ 7.47 (d, 2H, J = 8.4 Hz, 2'- and 6'-H),

(s, 1H, 3-CH₂OH), 3.46 (d, 2H, *J* = 6.4 Hz, 5-CH₂CH), 3.33 (d, 2H, *J* = 6.8 Hz, 3'-CH₂CH), 2.37 (s, 1H, 3-CH₂OH). ¹³C NMR (400 MHz, CDCl₃): δ 153.9, 150.1, 137.7, 136.2, 131.8, 131.2, 130.2, 129.5, 128.6, 128.5, 127.7, 126.2, 125.9, 116.7, 116.2, 115.7, 63.6, 39.4, 35.1. HRMS [*M* + Na]⁺ calcd 319.1310; found 319.1317.

3',5-Diallyl-3,5'-bis(hydroxymethyl)biphenyl-2,4'-diol (**11b**). Yield 70.4%. ¹H NMR (400 MHz, CDCl₃): δ 7.20 (d, 1H, *J* = 7.20 Hz, 2'-H), 7.03 (d, 1H, *J* = 7.0 Hz, 6'-H), 6.97 (d, 1H, *J* = 2.0 Hz, 6-H), 6.89 (d, 1H, *J* = 2.0 Hz, 4-H), 5.88–6.08 (m, 2H, 5-CH=CH₂ and 3'-CH=CH₂), 5.03–5.16 (m, 4H, 5-CH=CH₂ and 3'-CH=CH₂), 4.82 (s, 1H, 3-CH₂OH), 4.75 (s, 1H, 5'-CH₂OH), 3.44 (d, 2H, *J* = 6.4 Hz, 5-CH₂CH), 3.31 (d, 2H, *J* = 6.8 Hz, 3'-CH₂CH), 2.80 (s, 1H, 3-CH₂OH), 2.60 (s, 1H, 5'-CH₂OH). ¹³C NMR (400 MHz, CDCl₃): δ 153.5, 150.0, 137.6, 136.5, 131.8, 130.7, 130.2, 128.8, 128.6, 127.7, 127.5, 126.8, 125.8, 124.9, 116.1, 115.7, 64.1, 63.5, 39.3, 34.2. HRMS [*M* + Na]⁺ calcd 349.1410; found 349.1420.

■ ASSOCIATED CONTENT

S Supporting Information. HPLC purity and chromatograms of honokiol analogues and derivatives. This material is available free of charge via the Internet at <http://pubs.acs.org>.

■ AUTHOR INFORMATION

Corresponding Author

*Phone: 86-28-85164063. Fax: 86-28-85164060. E-mail: lijuan17@hotmail.com.

Author Contributions

[†]These authors contributed equally.

■ ACKNOWLEDGMENT

We are grateful to the National Key Programs of China during the 11th Five-Year Plan Period (2009ZX09501-015).

■ ABBREVIATIONS LIST

EC, endothelial cell; flk-1, fetal liver kinase-1; GFP, green fluorescent protein; NLS, nuclear localization signal; flt-1, friend leukemia integration-1; SAR, structure–activity relationship; DMSO, dimethylsulfoxide; IC₅₀, half-maximum inhibitory concentration; EDG, electron-donating group; EWG, electron-withdrawing group; HUVEC, human umbilical vein endothelial cell; A549, human lung carcinoma; HepG2, human hepatocellular liver carcinoma; LL/2, Lewis lung carcinoma; HPLC, high performance counter-current chromatography; MTT, (3-(4,5-dimethylthiazol-2-yl)-2,5-diphenyltetrazolium bromide; DMEM, Dulbecco's modified eagle medium; VEGF, vascular endothelial growth factor; FGF, fibroblast growth factor

■ REFERENCES

- (1) Carmeliet, P.; Jain, R. K. Angiogenesis in cancer and other diseases. *Nature* **2000**, *407*, 249–257.
- (2) Ferrara, N.; Kerbel, R. S. Angiogenesis as a therapeutic target. *Nature* **2005**, *438*, 967–74.
- (3) Carmeliet, P. Angiogenesis in health and disease. *Nature Med.* **2003**, *9*, 653–660.
- (4) Schmidt, J. M.; Tremblay, G. B.; Pagé, M.; Mercure, J.; Feher, M.; Dunn-Dufault, R.; Peter, M. G.; Redden, P. R. Synthesis and evaluation of a novel nonsteroidal-specific endothelial cell proliferation inhibitor. *J. Med. Chem.* **2003**, *46*, 1289–1292.

(5) Nüsslein-Volhard, C.; Dahm, R. *Zebrafish: A Practical Approach*; Oxford University Press: Oxford, 2002; pp 1–5.

(6) Feitsma, H.; Cuppen, E. Zebrafish as a Cancer Model. *Mol. Cancer Res.* **2008**, *6*, 685–694.

(7) (a) Hill, A. J.; Teraoka, H.; Heideman, W.; Peterson, R. E. Zebrafish as a model vertebrate for investigating chemical toxicity. *Toxicol. Sci.* **2005**, *86*, 6–19. (b) Blum, Y.; Belting, H. G.; Ellertsdottir, E.; Herwig, L.; Lüders, F.; Affolter, M. Complex cell rearrangements during intersegmental vessel sprouting and vessel fusion in the zebrafish embryo. *Dev. Biol.* **2008**, *316*, 312–322. (c) Lawson, N. D.; Weinstein, B. M. In vivo imaging of embryonic vascular development using transgenic zebrafish. *Dev. Biol.* **2002**, *248*, 307–318.

(8) St Croix, B.; Rago, C.; Velculescu, V.; Traverso, G.; Romans, K. E.; Montgomery, E.; Lal, A.; Riggins, G. J.; Lengauer, C.; Vogelstein, B.; Kinzler, K. W. Genes expressed in human tumor endothelium. *Science* **2000**, *289*, 1197–1202.

(9) The Angiogenesis Foundation. URL: <http://www.angio.org>.

(10) Madhusudan, S.; Harris, A. L. Drug inhibition of angiogenesis. *Curr. Opin. Pharmacol.* **2002**, *2*, 403–414.

(11) Staton, C. A.; Brown, N. J.; Reed, M. W. R. Current status and future prospects for antiangiogenic therapies in cancer. *Exp. Opin. Drug Discovery* **2009**, *4*, 961–979.

(12) Bai, X.; Cerimele, F.; Ushio-Fukai, M.; Waqas, M.; Campbell, P. M.; Govindarajan, B.; Der, C. J.; Battle, T.; Frank, D. A.; Ye, K.; Murad, E.; Dubiel, W.; Soff, G.; Arbiser, J. L. Honokiol, a small molecular weight natural product, inhibits angiogenesis in vitro and tumor growth in vivo. *J. Biol. Chem.* **2003**, *278*, 35501–35507.

(13) Chen, F.; Wang, T.; Wu, Y. F.; Gu, Y.; Xu, X. L.; Zheng, S.; Hu, X. Honokiol: A potent chemotherapy candidate for human colorectal carcinoma. *World J. Gastroenterol.* **2004**, *10*, 3459–3463.

(14) (a) Amblard, F.; Govindarajan, B.; Lefkove, B.; Rapp, K. L.; Detorio, M.; Arbiser, J. L.; Schinazi, R. F. Synthesis, cytotoxicity, and antiviral activities of new neolignans related to honokiol and magnolol. *Bioorg. Med. Chem. Lett.* **2007**, *17*, 4428–4431. (b) Fukuyama, Y.; Nakade, K.; Minoshima, Y.; Yokoyama, R.; Zhai, H.; Mitsumoto, Y. Neurotrophic activity of honokiol on the cultures of fetal rat cortical neurons. *Bioorg. Med. Chem. Lett.* **2002**, *12*, 1163–1166. (c) Esumi, T.; Makado, G.; Zhai, H.; Shimizu, Y.; Mitsumoto, Y.; Fukuyama, Y. Efficient synthesis and structure–activity relationship of honokiol, a neurotrophic biphenyl-type neolignan. *Bioorg. Med. Chem. Lett.* **2004**, *14*, 2621–2625. (d) Schühly, W.; Hüfner, A.; Pferschy-Wenzig, E. M.; Prettnner, E.; Adams, M.; Bodensieck, A.; Kunert, O.; Oluwemimo, A.; Haslinger, E.; Bauer, R. Design and synthesis of ten biphenyl-neolignan derivatives and their in vitro inhibitory potency against cyclooxygenase-1/2 activity and 5-lipoxygenase-mediated LTB₄-formation. *Bioorg. Med. Chem.* **2009**, *17*, 4459–4465. (e) Kong, Z. L.; Tzeng, S. C.; Liu, Y. C. Cytotoxic neolignans: an SAR study. *Bioorg. Med. Chem. Lett.* **2005**, *15*, 163–166.

(15) Luo, Y. F.; Xu, Y. B.; Chen, L. J.; Hu, J.; Peng, C.; Xie, D. C.; Shi, J. Y.; Huang, W. C.; Xu, G. B.; Peng, M.; Han, J.; Li, R.; Yang, S. Y.; Wei, Y. Q. Semi-synthesis and antiproliferative activity evaluation of novel analogs of honokiol. *Bioorg. Med. Chem. Lett.* **2009**, *19*, 4702–4705.

(16) Zhu, W.; Fu, A. F.; Hu, J.; Wang, T. E.; Luo, Y. F.; Peng, M.; Ma, Y. H.; Wei, Y. Q.; Chen, L. J. 5-Formylhonokiol exerts anti-angiogenesis activity via inactivating the ERK signaling pathway. *Exp. Mol. Med.* **2011**, *43*, 146–152.

(17) (a) Denton, R. M.; Scragg, J. T.; Galofre, A. M.; Gui, X. C.; Lewis, W. A concise synthesis of honokiol. *Tetrahedron* **2010**, *66*, 8029–8035. (b) Chen, C. M.; Liu, Y. C. A concise synthesis of honokiol. *Tetrahedron Lett.* **2009**, *50*, 1151–1152.

(18) Shi, J.; Xu, G. B.; Peng, A. H.; Peng, M.; Ye, H. Y.; Zhong, S. J.; He, S. C.; Li, S. C.; Luo, Y. F.; Wei, Y. Q.; Chen, L. J. Purification of honokiol derivatives from one-pot synthesis by high-performance counter-current chromatography. *J. Chromatogr. A* **2010**, *1217*, 3461–3465.

(19) Rocke, J.; Lees, J.; Packham, L.; Chico, T. The Zebrafish as a Novel Tool for Cardiovascular Drug Discovery. *Recent Pat. Cardiovasc. Drug Discovery* **2009**, *4*, 1–5.

(20) Lee, S. K.; Chun, H. K.; Yang, J. Y.; Han, D. C.; Son, K. H.; Kwon, B. M. Inhibitory effect of obovatal on the migration and invasion

of HT1080 cells via the inhibition of MMP-2. *Bioorg. Med. Chem.* **2007**, *15*, 4085–4090.

(21) Keshet, E.; Ben-Sasson, S. A. Anticancer drug targets: approaching angiogenesis. *J. Clin. Invest.* **1999**, *104*, 1497–1501.

(22) Folkman, J.; Hahmfeldt, P.; Hlatky, L. Cancer: looking outside the genome. *Nature Rev. Mol. Cell. Biol.* **2000**, *1*, 76–79.

(23) Abdollahi, A.; Folkman, J. Evading tumor evasion: current concepts and perspectives of anti-angiogenic cancer therapy. *Drug Resist. Update* **2010**, *13*, 16–28.